

# Free-Form Mirror Design Inspired by Photometric Stereo

Kazuaki Kondo, Yasuhiro Mukaigawa, and Yasushi Yagi

The Institute of Scientific and Industrial Research, Osaka University, Japan  
{kondo, mukaigaw, yagi}@am.sanken.osaka-u.ac.jp

**Abstract.** A significant issue in the design of catadioptric imaging systems is what shape the component mirrors should take. In this paper, we propose a novel algorithm for designing a free-form mirror. A free-form mirror expressed as the assembly of its gradients, is the most flexible surface representation that can form various shapes. We improve the shape reconstruction framework used in a photometric stereo scheme for use in the design of free-form mirrors for catadioptric imaging systems. An optimal mirror shape is created to produce the best possible desired projection, under integrability conditions in order to be a consistent surface. Curved mirrors are designed for various catadioptric configurations and these design experiments confirm that the resulting free-form mirrors can approximate the desired projections.

## 1 Introduction

Catadioptric imaging systems combine cameras with mirrors to change camera projections. These systems are used in numerous applications, including robot navigation and wide view surveillance. Conventional catadioptric imaging systems use mirrors with basic shapes [1, 2], or with special rotationally symmetric shapes to obtain the desired resolution in a vertical direction [3–6]. Gaechter et al. used not only a such mirror also a space variant imager to control image resolution[9]. Kondo et al. designed an asymmetric convex mirror to obtain an isotropic projection property [7]. Hicks et al. assumed a mirror formed by a polynomial function, and solved it using a non-linear optimization [8]. The shapes of all the mirrors used in these proposals were defined by a parameterized function, resulting in limited shape representation and projection forming capabilities. A generalized representation of a mirror surface with a high DOF, together with the knowledge of the design thereof, are necessary to produce arbitrary projections.

A free-form mirror determined from multiple control points is one of the most generalized representations. It can be used to realize, without distortion, various projections given by practical configurations, such as a wide panoramic view. In this case, the desired projection is a uniform projection onto a cylindrical scene around the camera. Another example of the use thereof is to correct the image distortion in a projector system. A free-form mirror can produce counter-warping against the distortion. An algorithm for designing free-form mirrors was proposed by Swaminathan et al. [10]. They modeled the shape of the mirror

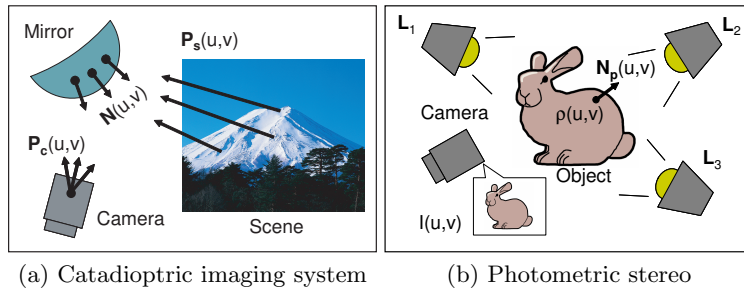


**Fig. 1.** Configuration of two problems. (a) Design of a single free-form mirror for a catadioptric imaging system. (b) Formation of photometric stereo schemes.

using the cross products of splines to formulate the design problem as a linear equation. A limited number of control points on the splines that decide the design DOF, however, still remain. In addition, this design cannot represent non-smooth surfaces.

In this paper, we propose a new design method for a free-form mirror constructed as the assembly of its gradients. This type of free-form definition can represent mirror shapes, including non-smooth surfaces, more generally than the conventional algorithms, thus allowing a variety of projections to be produced. An example of this is a compound mirror constructed from multiple flat planes such as a polygon mirror. Of course compound mirrors constructed from curved surfaces can be defined as a result of the free-form definition. Our method can design such a compound mirror directly as it is a single mirror surface.

However, there is a problem in using a free-form mirror surface. The gradients of the points are determined so as to satisfy a given desired projection, but their movement is actually not perfectly independent as they must form a consistent surface. In this case, the gradients need to move under the constraint known as integrability. This problem also occurs in photometric stereo schemes for shape reconstruction, where the optimal shape of a target object forming shadings in an input image is estimated. The free-form mirror design algorithm estimates the optimal shape of a mirror that produces a given projection. These two problem specifications are therefore very similar. However, using the methods deployed in photometric stereo schemes directly is not feasible in that the meaning of the residuals is different in each case. The assumption of an orthographic camera is also a problem in catadioptric imaging systems. To this end, the algorithms used in photometric stereo schemes are extended for application to the mirror design problem. The results are tested experimentally.

## 2 Problem settings

### 2.1 Problem specification for mirror design

Mirror design for catadioptric imaging systems begins with defining the desired projection. Assume that each incoming ray from a scene is reflected at some

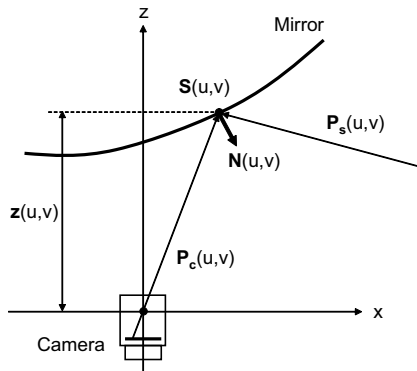


**Fig. 2.** Camera-Mirror configuration.

point on the free-form surface, and its captured position on the image plane is  $(u, v)$ . Then the desired projection can be expressed by rays in the scene  $\mathbf{P}_s(u, v)$  defined on the image plane, and can be freely manipulated by a designer. Similarly, projections of the primary camera are expressed as  $\mathbf{P}_c(u, v)$ . Figure 1(a) and Fig. 2 illustrate this configuration.  $\mathbf{P}_s(u, v)$  and  $\mathbf{P}_c(u, v)$  are defined on the image plane where all lengths are equal to 1. These two vector fields are related by reflection on a curved mirror placed in front of the camera:

$$\mathbf{N}(u, v) = -\frac{\mathbf{P}_s(u, v) + \mathbf{P}_c(u, v)}{\|\mathbf{P}_s(u, v) + \mathbf{P}_c(u, v)\|} \quad (1)$$

where  $\mathbf{N}(u, v)$  is a normal vector field. The aim in mirror design is to determine the surface that produces  $\mathbf{N}(u, v)$ . This is achieved by integrating gradient vectors from the normal vector field  $\mathbf{N}(u, v)$ .

Generally, gradients of a smooth surface can be determined by differentiation. However, the inverse, integrating the given gradients to reconstruct an original surface, is not always possible. Since an integration result depends on its path, integrations along different paths may (and in most cases do) produce divergent results when freely distributed gradients are given. To form a consistent surface, one needs to consider this problem.

## 2.2 Problem specification for formulation of photometric stereo schemes

The creation of photometric stereo schemes can be seen as a similar problem to mirror design. Photometric stereo schemes reconstruct a surface in two steps. First, a normal vector field of the target object is estimated from images under different illuminations. The formulation of the general image irradiance equation for classical photometric stereo schemes given below assumes that  $(x(u, v), y(u, v), z(u, v))$  is the form of the object surface defined on the image plane of a camera  $(u, v)$ .

$$I(u, v) = \rho(u, v) \frac{\mathbf{L} \cdot \mathbf{N}(u, v)}{\|\mathbf{L}\| \|\mathbf{N}(u, v)\|} \quad (2)$$

where  $I(u, v)$  is the intensity at  $(u, v)$ ,  $\rho(u, v)$  is the albedo,  $\mathbf{L}$  is the direction of the parallel light source, and  $\mathbf{N}(u, v)$  is the normal vector of the object surface (Fig. 1(b)). Parallel light sources illuminating from three or more different points allow us to solve Eq. (2) about one normal vector and obtain a normal vector field.

The gradients produced by the normal vector field are then integrated to reconstruct the shape of the original object. Various methods have been proposed to assist in this process. These include solving a two-dimensional Poisson equation (this is the easiest and the most popular), an iterative approach with the Gauss-Seidel method as per Horowitz et al. [11], and a linear method from Agrawal [12].

### 2.3 Similarities and differences in problem specification

As described in Sections 2.1 and 2.2, despite mirror design and photometric stereo scheme creation being very different projects, interestingly, they result in very similar problems. We make use of this similarity in this paper. However, using the same approach as in photometric stereo scheme creation has disadvantages for mirror design.

Normal vector fields estimated from input images in the photometric stereo schemes are generated from a real object. So, in principle, the shape of the object surface can be perfectly reconstructed if the images do not include any errors. Thus, if the integration cannot be performed consistently, it is as a result of image errors caused by, for instance, specular reflections, shadows, miscalibration, bad approximations, and so on. Decreasing the influence of image errors is, therefore, important in this type of shape reconstruction problem.

For mirror design, whether or not the normal vector field produced from the desired projection  $\mathbf{P}_s(u, v)$  can form a continuous consistent surface is a problem. Generally the desired projection  $\mathbf{P}_s(u, v)$  is given without considering the possibility of forming a consistent surface. Therefore, in most cases a solution that perfectly satisfies a given desired projection  $\mathbf{P}_s(u, v)$  does not exist, which is very different from the shape reconstruction problem in photometric stereo schemes. The reason why integration of the gradients does not form a consistent surface is the given projection itself. In this case an approach that minimizes the overall projection residual is recommended.

Furthermore some photometric stereo schemes assume a known boundary condition and an orthographic projection camera. In free-form mirror design, the shape of the mirror is completely unknown. Furthermore, since the mirror is placed close to the camera in catadioptric imaging systems, orthographic projection cannot be assumed. The mirror design problem for catadioptric imaging systems requires a method without boundary conditions for conventional perspective projection cameras. Thus, the approach in photometric stereo schemes needs to be extended for use in mirror design.

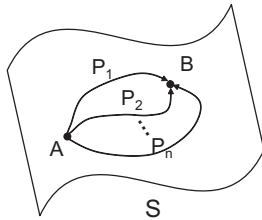


**Fig. 3.** A model of integrability on a surface. Integration results from  $A$  to  $B$  along any path  $P_i$  are constant for a consistent surface.

### 3 Design of a free-form mirror

#### 3.1 Representation of the free-form mirror

In this paper we assume that a target catadioptric imaging system is constructed with a conventional perspective camera  $C$  and a single reflective mirror  $M$  placed in front of the camera (Fig. 2). The camera  $C$  has a  $W \times H$  size image plane  $(u, v)$  that corresponds to a pixel on the image plane. The camera projection vector field  $\mathbf{P}_c(u, v)$  is given by:

$$\mathbf{P}_c(u, v) = \begin{bmatrix} -K_u u \\ -K_v v \\ f \end{bmatrix} \quad (3)$$

where the camera has a focal length  $f$  and the size of the pixels  $K_u, K_v$ . We assume a depth of field  $z(u, v)$  defined on the image plane to form the shape of the mirror surface  $\mathbf{S}(u, v)$ :

$$\mathbf{S}(u, v) = \frac{1}{f} \mathbf{P}_c(u, v) z(u, v). \quad (4)$$

We represent the free-form mirror shape with gradients  $p = \frac{\partial z}{\partial u}, q = \frac{\partial z}{\partial v}$ . The objective of mirror design is to optimize  $\mathbf{S}(u, v)$  by moving  $p, q$  so as to produce  $\mathbf{N}(u, v)$  with a minimum residual.

#### 3.2 Integrability of a free-form surface

The reconstruction or design of a 3D surface must be done in such a way as to form a consistent surface. This is an implicit constraint that is referred to as the integrability of the surface [13]. On a consistent surface, integration of surface gradient vectors from a point  $A$  to a point  $B$  must be constant along any path as shown in Fig. 3. This is known as the integrability of a potential field [13]. When an integration result along a path differs from that along any other path, the surface is discontinuous at that point.

Let  $\mathbf{p}(u, v)$  and  $\mathbf{q}(u, v)$  be gradients of  $\mathbf{S}(u, v)$  in the  $u$  and  $v$  directions  $\frac{\partial \mathbf{S}}{\partial u}$  and  $\frac{\partial \mathbf{S}}{\partial v}$ , respectively. Integrability of the surface is generally formulated with a curl operator of  $\mathbf{S}$  as:

$$\mathbf{curl}(\mathbf{p}, \mathbf{q}) = \frac{\partial \mathbf{p}}{\partial v} - \frac{\partial \mathbf{q}}{\partial u} = \mathbf{0} \quad (5)$$

at any point on  $(u, v)$ , thus representing the constraint of forming a consistent surface. Note that the shape of the mirror surface is as per Eq. (4). Since camera projection  $\mathbf{P}_c$  is determined by the camera parameters, and the only freedom in the shape  $\mathbf{S}(u, v)$  is in the scalar field  $z(u, v)$ , an integrability constraint can be written in a scalar domain about  $z$  instead of a vector domain  $\mathbf{S}$ :

$$\text{curl}(p, q) = \frac{\partial p}{\partial v} - \frac{\partial q}{\partial u} = 0. \quad (6)$$

The mirror design must be performed with Eq. (6) to form a consistent surface.

The integrability constraint is enforced over a discrete domain based on [12] to formulate the design problem as linear equations. The mirror surface can then be described more generally in a discrete domain than in a spline defined surface as proposed in [10] or a polynomial function as proposed in [8]. In a discrete domain, the derivatives of the gradients are given by:

$$\begin{aligned} \frac{\partial p}{\partial v} &= p(u, v+1) - p(u, v) \\ \frac{\partial q}{\partial u} &= q(u+1, v) - q(u, v). \end{aligned} \quad (7)$$

The equation for curl can be written in the discrete domain using Eq. (7):

$$\text{curl} = p(u, v+1) - p(u, v) - q(u+1, v) + q(u, v). \quad (8)$$

One can write Eq. (8) in linear form as:

$$\text{curl} = [1\dots -1\dots 1\dots -1]\mathbf{g} \quad (9)$$

where  $\mathbf{g}$  is a  $WH \times 1$  vector constructed from the series of gradients  $p, q$ . Eq. (8) corresponds to a particular loop integral around a box of four pixels. Note that the loop integral around any other bigger loop can be expressed as linear combinations of the elementary loop integrals and thus does not provide any additional information. Thus stacking Eq. (9)=0 on the entire  $(u, v)$  field, one obtains a linear equation for the integrability constraint.

$$\mathbf{C}\mathbf{g} = \mathbf{0} \quad (10)$$

$\mathbf{C}$  is a sparse matrix of size  $(W-1)(H-1) \times 2WH$ . Each row in  $\mathbf{C}$  is in accordance with Eq. (9) and has four non-zero values; two +1's corresponding to  $p(u, v+1)$  and  $q(u, v)$ , respectively, and two -1's corresponding to  $p(u, v)$  and  $q(u+1, v)$ , respectively.

### 3.3 Integrability on a perspective projection

The majority of research into photometric stereo schemes has assumed an orthographic projection camera because a camera can be placed sufficiently far

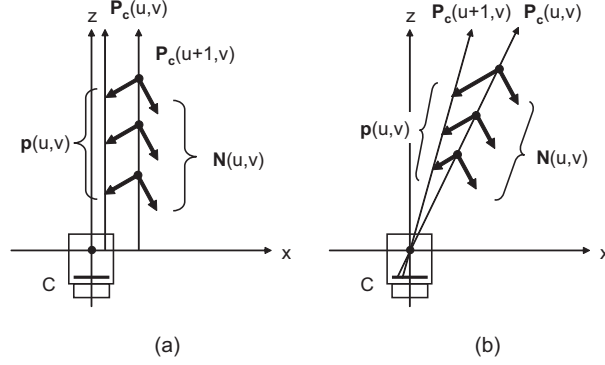


**Fig. 4.** Relationship between a normal vector and a gradient vector. (a) and (b) show models of orthographic projection and perspective projection cameras. The gradient vector in (a) is constant, independent of its depth. In (b) depth is ambiguous.

from the target object to approximate the perspective projection into an orthographic one. If an orthographic projection is assumed, we can easily calculate the gradients  $p, q$  from the normal vector field  $\mathbf{N}$  because  $x = K_u u, y = K_v v$  (Fig. 4(a)). However, in catadioptric imaging systems, curved mirrors are placed relatively close to the camera for compactness. Thus, the perspective projection cannot be approximated to an orthographic one. This means a method is needed to calculate the gradients.

Generally a normal vector  $\mathbf{N}$  can be decomposed into two perpendicular gradient vectors whose outer product becomes  $\mathbf{N}$  itself. For a perspective projection, we can obtain the directions of the gradient vectors, but their lengths are not uniquely determined because they depend on their depth as shown in Fig. 4(b). Tankus' proposal [14, 15] provides a hint to solve this problem. Fortunately, the relationship between the length of the gradient vector and its depth under perspective projection is linear, resulting in

$$\begin{aligned} p' &= \frac{1}{z} \frac{\partial z}{\partial u} \\ q' &= \frac{1}{z} \frac{\partial z}{\partial v} \end{aligned} \quad (11)$$

rather than  $p = \frac{\partial z}{\partial u}$  and  $q = \frac{\partial z}{\partial v}$ .

Having obtained the above, consideration should be given to how the integrability constraint with  $p', q'$  is formulated. Consider that  $\text{curl}(p', q')$  can be expressed with  $\text{curl}(p, q)$  as:

$$\begin{aligned} \text{curl}(p', q') &= \frac{\partial p'}{\partial v} - \frac{\partial q'}{\partial u} \\ &= \frac{\partial}{\partial v} \left( \frac{1}{z} \frac{\partial z}{\partial u} \right) - \frac{\partial}{\partial u} \left( \frac{1}{z} \frac{\partial z}{\partial v} \right) \\ &= -\frac{1}{z^2} \left( \frac{\partial z}{\partial v} \frac{\partial z}{\partial u} - \frac{\partial z}{\partial u} \frac{\partial z}{\partial v} \right) + \frac{1}{z} \left( \frac{\partial^2 z}{\partial v \partial u} - \frac{\partial^2 z}{\partial u \partial v} \right) \\ &= \frac{1}{z} \text{curl}(p, q) \end{aligned} \quad (12)$$

Since  $z > 0$ ,  $\text{curl}(p, q) = 0$  is equivalent to  $\text{curl}(p', q') = 0$ . We can now say that curls in the discrete domain have the same characteristics as curls in the

continuous domain. Thus a line of  $p', q'$  can be used as  $\mathbf{g}$  instead of  $p, q$  for the integrability constraint. Note that this usage of  $p', q'$  requires an additional step: forming the shape. The shape of the surface can easily be produced by integrating  $p, q$ . Integration of  $p', q'$  provides a log scaled shape for the radical shape because

$$\begin{aligned} p' &= \frac{1}{z} \frac{\partial z}{\partial u} = \frac{\partial \ln z}{\partial u} \\ q' &= \frac{1}{z} \frac{\partial z}{\partial v} = \frac{\partial \ln z}{\partial v}. \end{aligned} \quad (13)$$

The exponents of the integration results must be obtained to convert a log scaled shape into a radical.

### 3.4 Gradient optimization under the integrability constraint

An optimal shape for the mirror surface should minimize residuals from the desired gradients under the integrability constraint from the previous section. The approach proposed by Agrawal [12] for the photometric stereo method uses a graph that describes the reliability of the gradients. Gradients with high reliability are retained and the others are ignored to satisfy the integrability constraint, much like an elimination of outliers. This proposal works well for the photometric stereo problem because the gradients obtained from the images can have unexpected errors. Conversely, residuals in the mirror design problem are not caused by unexpected errors but by non-integrability of the given desired gradients. Thus, minimization of residuals all over is superior to the elimination of outliers.

We use a simple Least Mean Square(LMS) algorithm to obtain the optimal gradients. Let  $\mathbf{g}$  be a line of gradients  $p', q'$  that form a surface, and  $\mathbf{g}_d$  be a line of desired gradients obtained from the desired projection. The ideal solution about  $\mathbf{g}$  is:

$$\mathbf{g} = \mathbf{g}_d. \quad (14)$$

If this equation is solved under integrability constraint Eq. (10), that contracts the solution space for Eq. (14), the solution space  $\mathbf{h}$  is given by:

$$\mathbf{g} = \mathbf{T}\mathbf{h}. \quad (15)$$

where  $\mathbf{T}$  is a  $2WH \times (W-1)(H-1)$  matrix whose rows are linear independent solutions of  $\mathbf{C}\mathbf{g} = \mathbf{0}$ . Since the matrix  $\mathbf{C}$  is very sparse, one can easily produce the  $\mathbf{T}$  matrix. Substituting Eq. (15) into Eq. (14) and solving it with the LMS algorithm, we obtain optimal solutions about gradients  $p', q'$ .

$$\mathbf{T}\mathbf{h} = \mathbf{g}_d \quad (16)$$

$$\mathbf{h} = \mathbf{T}^+ \mathbf{g}_d \rightarrow \mathbf{g} = \mathbf{T}\mathbf{T}^+ \mathbf{g}_d \quad (17)$$

where  $\mathbf{T}^+$  is a pseudo inverse matrix of  $\mathbf{T}$ . This procedure does not require any additional conditions despite the fact that the photometric stereo scheme needs boundary conditions.

## 4 Designing experiments

We performed design experiments to validate the effectiveness of our algorithm with different configurations. How much a desired projection is realized depends on the integrability of the desired projection. In the following three configurations, the former two require producing non-integrable projections. Since there is no form that perfectly satisfies the projection, there is no ground truth. The last configuration requires producing integrable one, we can evaluate and compare degree of approximations given by our algorithm and the conventional one.

### 4.1 Wide panoramic imaging system

The free-form mirrors designed with our algorithm satisfy both the expanding FOV and reduced distortion on captured images. We assumed a configuration for a wide panoramic imaging system as shown in Fig. 5(a). In this setup, distortion-free means that cylindrical scenes around the camera appear directly on the images. A desired projection is given by dividing an objective panoramic FOV into the same size grids. The FOV of the camera and the objective panoramic FOV are respectively,  $\pm 20.0 \times \pm 15.3 \text{degrees}$  produced with a  $6.0 \text{mm}$  focal length and  $\pm 50.0 \times \pm 20.0 \text{degrees}$ . The shape of the designed mirror, a target panoramic scene, and a captured image are shown in Fig. 5. Checkers on the cylindrical scene appear approximately as squares on the image. The center region has almost no distortion, whereas a little distortion appears at the image edges. The distortion is, however, much smaller than that in the conventional parametric approaches such as with rotationally symmetric mirrors.

### 4.2 Catadioptric projector system

Free-form mirrors can also correct image distortions in projector systems. Generally direct projection by an upward facing projector has trapezoidal distortion. Using a combination of a projector and a free-form mirror, rectangular images appear on a screen without image deformation, and these cancel the trapezoidal distortion. Since the projection of a projector is the same as that of a camera apart from the direction of the light, our algorithm can be applied directly. Assume a catadioptric projector system as shown in Fig. 6(a). We configured a rectangular projection as the desired one, and designed the catadioptric projector system using our algorithm. The focal length and FOV of the projector are the same as those of the camera in the previous experiment. The shape of the designed mirror and examples of the projected images are shown in Fig. 6(b) and Fig. 6(c-e), respectively. A trapezoidal distorted image from only the upward facing projector is corrected to a rectangular image with the designed free-form mirror. Although a little distortion still remains, the amount of image deformation required to cancel it is much smaller.

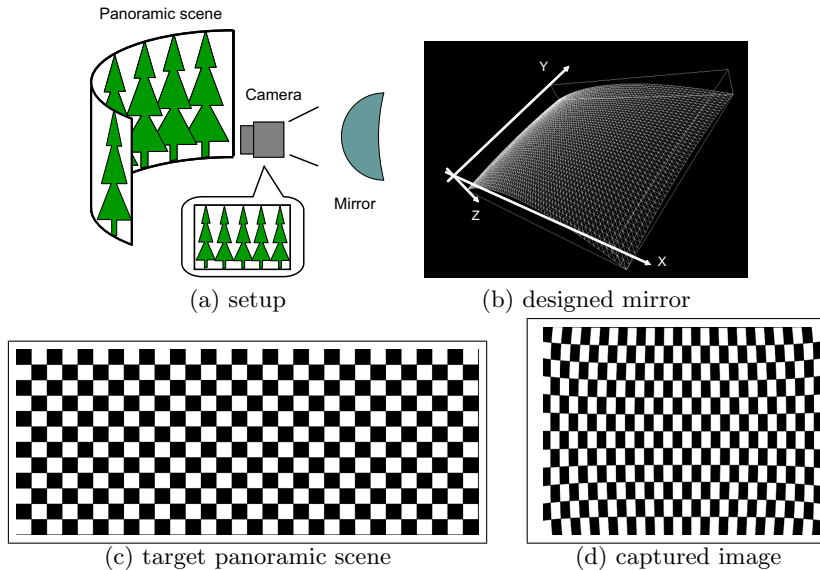


**Fig. 5.** Wide panoramic imaging system.  $X$ ,  $Y$ , and  $Z$  axes in figure (b) correspond to the camera coordinate system.

### 4.3 Compound Mirror

Direct definition of the mirror surface with its gradients as control variables can represent a non-smooth surface. So our method covers not only a single curved mirror addressed in conventional methods such as [8, 10] but also a compound mirror constructed by multiple component mirrors. In this section, we evaluate the design ability for a compound mirror by designing a pyramid mirror. The pyramid mirror is constructed from four flat mirrors, which have four non-smooth borders at their joints. Thus many residuals remain when redesigning the pyramid mirror shape from its own projection using the conventional method [10] that assumes a single curved mirror (Fig. 7 right). In order to avoid these residuals, each component mirror needs to be designed individually in the conventional methods. But this causes problems in the construction step as continuity at the joints is not considered. On the other hand, our method suppresses residuals at the joints and allows them to expand to neighborhoods (Fig. 7 left) in spite of the single mirror design. The pyramid mirror, which is one of the simplest examples of compound mirrors, is used to evaluate residuals easily. Our method also works well for other compound mirrors, such as the construction of curved mirrors.

## 5 Conclusion

In this paper, we proposed a novel design method for a free-form mirror surface for a catadioptric imaging system using the assembly of its gradients. We for-

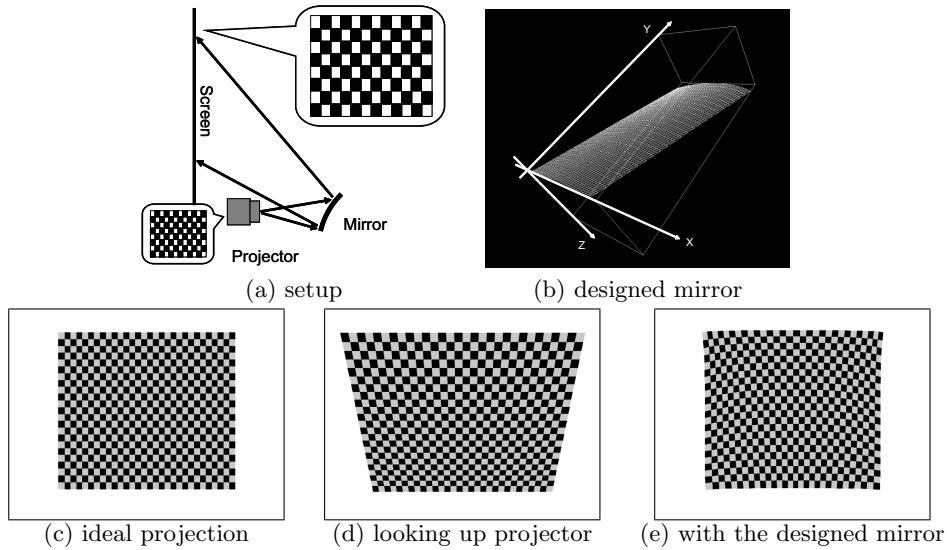


**Fig. 6.** Catadioptric projector system.

mulated an integrability constraint of the gradients to form a consistent surface in the mirror design, using a method similar to that used in creating photometric stereo schemes. Our approach produces mirror surfaces with minimal overall projection residuals, and it also works well for compound mirrors.

This work is supported by the Special Coordination Funds for Promoting Science and Technology of Ministry of Education, Culture, Sports, Science and Technology.

## References

1. K. Yamazawa, Y. Yagi, and M. Yachida, “HyperOmni Vision: Visual Navigation with an Omnidirectional Image Sensor”, *Systems and Computers in Japan*, Vol. 28, No. 4, pp. 36-47, 1997.
2. S. K. Nayar, “Catadioptric Omnidirectional Camera”, *Proc. of IEEE Conference on Computer Vision and Pattern Recognition (CVPR)*, pp. 482-488, 1997.
3. T. Nakamura and H. Ishiguro, “Automatic 2D map construction using a special catadioptric sensor”, *Proc. of IEEE/RSJ Int. Conf. on Intelligent Robots and Systems (IROS)*, pp. 196-201, 2002.
4. J. Gasper, C. Decco, J. Okamoto and J. S. Victor, “Constant Resolution Omnidirectional Cameras”, *Proc. of IEEE Workshop on Omnidirectional Vision (OMNIVIS)*, pp. 27-34, 2002.
5. T. L. Conroy and J. B. Moore, “Resolution Invariant Surfaces for Panoramic Vision Systems”, *Proc. of IEEE Int. Conf. on Computer Vision (ICCV)*, Vol. 1, pp. 392-397, 1999.
6. R. A. Hicks and R. K. Perline, “Equi-areal Catadioptric sensors”, *Proc. of IEEE Workshop on Omnidirectional Vision (OMNIVIS)*, pp. 13-19, 2002.

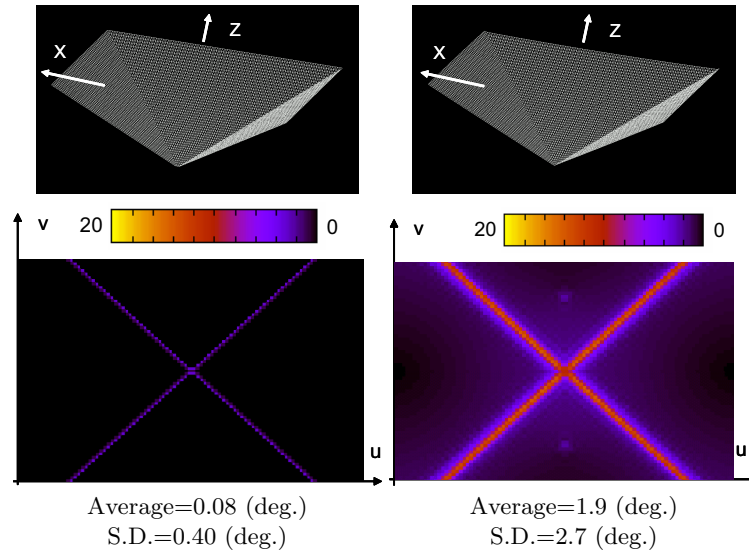


**Fig. 7.** Mirror design for discontinuous projection. (Left) our algorithm. Error spreading is kept to narrow areas. The number of the projection errors is small. (Right) Swaminathan’s algorithm. Errors spread in bands around the boundaries.

7. K. Kondo, Y. Yagi, and M. Yachida, “Non-isotropic Omnidirectional Imaging System for an Autonomous Mobile Robot”, Proc. of IEEE International Conference on Robot and Automation (ICRA), 2005.
8. R. A. Hicks, “Designing a mirror to realize a given projection”, Journal of Optical Society of America, Vol. 22, No. 2, pp. 323-329, 2005.
9. S. Gaechter, T. Pajdla, and B. Micusik, “Mirror Design for an Omnidirectional camera with a space variant imager”, Proc. of IEEE Workshop on Omnidirectional Vision Applied to Robotic Orientation and Nondestructive Testing, pp. 99-105, 2001.
10. R. Swaminathan, S. K. Nayar, and M. D. Grossberg, “Designing of Mirrors for catadioptric systems that minimize image error”, Proc. of IEEE Workshop on Omnidirectional Vision (OMNIVIS), 2004.
11. I. Horowitz and K. Kiryati, “Depth from gradient fields and control points: Bias correction in photometric stereo”, Journal of Image and Vision Computing, Vol. 22, No. 9, pp. 681-694, Aug., 2004.
12. A. Agrawal and R. Rasker, “An Algebraic Approach to Surface Reconstruction from Gradient Fields”, Proc. of IEEE Int. Conf. on Computer Vision (ICCV), Vol. 1, pp. 174-181, 2005.
13. B. K. P. Horn, “Robot Vision(Mit Electrical Engineering and Computer Scenece Series)”, Mit Pr.
14. A. Tankus, N. Sochen, and Y. Yeshurun, “A New Perspective [on] Shape-from-Shading”, Proc. of IEEE Int. Conf. on Computer Vision (ICCV), Vol. 2, pp. 862-869, 2003.
15. A. Tankus and N. Kiryati, “Photometric Stereo under Perspective Projection”, Proc. of IEEE Int. Conf. on Computer Vision (ICCV), Vol. 1, pp. 611-616, 2005.